STUDY OF Zn-Fe AND Zn-Fe-Co ALLOYS COATINGS OBTAINED BY ELECTRODEPOSITION FROM ACID BATHS CONTAINING CITRATE IONS[1]

Roberto Zenhei Nakazato[2]
Flávia Cristina Zenith Ferreira[3]
Conceição Aparecida Matsumoto Dutra[2]
Eduardo Norberto Codaro[2]

Abstract

Zinc alloy coatings have attracted great interest in industry due to the characteristics of ductility, weldability, adhesion to paint and corrosion resistance in comparison with pure zinc. In this work, Zn-Fe alloy and Zn-Co-Fe were obtained on copper from acid baths containing citrate. The electrochemical experiments were performed on 0.5 mol/L Na_2SO_4 + 0.05 mol/L EDTA solution. Results of anodic dissolution voltammetry and galvanostatic dissolution showed that the decrease in $[Zn^{+2}]$ in the bath results in electrodeposited Zn-Fe with higher Fe content (1.2 - 60%) when the ratio $[Zn^{2+}]:[Fe^{2+}]$ change from 1:1 to 1:4. Analysis of scanning electron microscopy with energy dispersive spectroscopy (SEM/EDS) and X-ray diffraction showed refinement of the structure up to loss of crystallinity in alloys with high Fe content and the presence of ZnFe η-phase in alloys with low Fe content. Addition of 0.05 mol/L Co^{2+} bath for different $[Zn^{+2}]$ and $[Fe^{+2}]$ favored the incorporation of Fe in the Zn-Fe-Co alloy. It was also observed that increasing the current density of -5 to -30 mA/cm^2 contributed to the increasing content of Fe in the alloy.
Key words: Zinc alloys; Electrodeposition; Zn-Fe alloy; Zn-Fe-Co alloy.

1 INTRODUCTION

The electrodeposits of zinc alloys have attracted a lot of interest in recent decades because they have shown higher corrosion resistance compared to pure zinc coatings, electroplated or galvanized by hot dip. Such coatings behave like sacrifice metals in relation to steel and protection occurs by providing a resistant and adhesive coating, hindering the contact of steel with the corrosive environment. If the coating is damaged and the steel is exposed, cathodic protection will take place and, also, barrier protection, since the zinc corrosion products, formed in the damaged area, will cover the exposed surface of the steel (1).

The growing interest in electrodeposited coatings is due to their superior properties, as they are more uniform, finer and, in some cases, bright. In hot dip zinc plating the layer thickness is irregular and poorly controlled.

In order to obtain coatings more resistant to corrosion, various researches have been developed involving the addition of elements such as Co, Ni, Fe, Sn and Cr, to the zinc electrodeposits, resulting in the formation of alloys on the substrate (2). These metals, when used as alloying elements, affect the reduction potential of the coating, approximating it to the potential of steel, slowing the dissolution, keeping it less active than the layer of pure zinc and increasing its lifetime. The incorporation of alloying elements, mainly, from the iron group (Fe, Co, Ni) to the zinc alloys gives good characteristics of ductility, weldability, adhesion to the paint and corrosion resistance (3). In Zn-Co alloys with only 1% of cobalt, it is possible to observe an improvement in the functional properties (4) and containing 30% cobalt anticorrosive properties are excellent, but the optimum content of alloying elements is still a matter of controversy (5).

Although binary alloys such as ZnFe, ZnCo have already been in use in the industry for some time, the ZnFeCo alloy is the most recent in the group of zinc alloys. The mechanism of electrodeposition of alloys belonging to this group still draws considerable academic interest, since according to Gómez (6), both the composition and morphology of these electrodeposits are very sensitive to variations in solution composition and to the electrochemical parameters used during the electrolysis. Furthermore, they show the unexpected phenomenon of anomalous codeposition, in which zinc, less noble metal is deposited preferably under various conditions of electrodeposition (7, 8).

In this work, the electrochemical behavior, morphology and the microstructure of Zn-Fe and Zn-Fe-Co electrodeposits prepared from acid baths containing citrate ions were studied.

2 METHODOLOGY

All the solutions were prepared with analytical grade chemicals and distilled water. The pH of the electrodeposition solutions was set at 3.5, based on studies preliminaries to ensure that there was no precipitation of hydroxides and adjusted by adding diluted HCl or KOH, as needed, and the measurements made with the aid of a pHmeter HANNA–pH21. The electrochemical tests were conducted with a conventional three-electrode cell. The working electrodes, Zn-Fe and Zn-Fe-Co alloys, were obtained on copper electrode with a geometric area of 0.28 cm^2. The graphite road was used as the counter electrode and the reference electrode was the saturated calomel electrode (SCE) Hg/Hg$_2$Cl$_2$, KCl$_{sat}$, (+242 mV vs. NHE), connected

via a Luggin capillary. The experiments were run using deaerated electrolyte 0.5 mol/L Na_2SO_4 + 0.05 mol/L EDTA, with bubbling N_2 gas during the tests at 25 °C. This solution was used to ensure total dissolution of the coating in potentiodynamic and galvanostatic tests and, since it is known that EDTA form soluble complexes with Zn^{2+}, Fe^{2+} or Fe^{3+} and preventing the formation of oxides on the electrode (9).

A potentiostat/galvanostat MICROQUÍMICA, MQPG-02 with MQ/12/8PCC interface containing cyclic voltammetry and chronopotentiometry programs was used in the tests. Copper was used as substrate, which was prepared by mechanical polishing with different grade emery paper up to 1500 mesh before each test. All the tests were done in triplicate to ensure reproducibility of the system.

In the study of variation of the ratios $[Zn^{2+}]/[Fe^{2+}]$ the electrodeposits were obtained from electroplating solution at the following concentrations: 0.40 mol/L $FeCl_2$, 0.10 mol/L citrate and 0.10 mol/L, 0.13 mol/L, 0.16 mol/L, 0.18 mol/L, 0.20 mol/L and 0.40 mol/L $ZnCl_2$ on the copper electrode, applying current densities of -15 mA/cm^2 and -20 mA/cm^2, whose range has change in the type of codeposition (3). The dissolution voltammograms were obtained at a scan rate of 5 mV s^{-1} in the potential range of -1.2 V to +0.2 V and the galvanostatic dissolution curves to +5 mA/cm^2 for 600 sec.

The electrochemical study for Zn-Fe-Co alloys were obtained from the same electroplating solution used for binary alloys just adding 0.05 mol/L $CoCl_2$ and changing the potential range from -1.2 V to 0.0 V in the anodic dissolution voltammetry test.

Copper plates, measuring 15 mm x 60 mm and 0.5 mm thick were used as substrate for electrodeposition and characterization of the coatings. These plates were mechanically polished with different grade emery paper up to 1500 mesh, rinsed with distilled water and cleaned with isopropyl alcohol in THORNTON ultrasound bath for 10 minutes and then dried. The copper plates were introduced into the electrochemical cell containing electroplating solution and a current density of –15 mA/cm^2 was applied to the system by 1200 sec. The samples were sectioned in 15 mm x 15 mm for the following tests: scanning electronic microscopy (SEM), in ZEISS microscope - EVO LS15, with probe OXFORD INSTRUMENTS-INCAx for X-ray scattering spectroscopy (EDS) and X-ray diffraction (XDR) in SHIMADZU XDR-6000 diffractometer.

3 RESULTS AND DISCUSSION

Study of Electrodeposits of Zn-Fe Alloys
The electrodeposits of Zn-Fe alloys were obtained on a copper substrate in electroplating solutions containing different concentrations of Zn^{2+} (0.10 mol/L, 0.13 mol/L, 0.16 mol/L, 0.18 mol/L, 0.20 mol/L and 0.40 mol/L), setting the concentrations of Fe^{2+} (0.40 mol/L) and citrate ions (0.10 mol/L). The electrolysis is performed at galvanostatic mode with a current density of -15 mA/cm^2.

Electrochemical Study
The results obtained using voltammetry of anodic dissolution, Figure 1, show curves I-E for the electrodeposits of Zn-Fe alloys under different conditions. Through the voltammograms it can be seen that for low $[Zn^{2+}]$ (0.10 mol/L and 0.13 mol/L, $[Zn^{2+}]/[Fe^{2+}]$ ratios 1:4 and 1:3, respectively) the current peaks are situated at approximately -0.57 V, close to the potential of pure iron. However, in $[Zn^{2+}]$ higher (0.16 mol/L and 0.20 mol/L, ratios $[Zn^{2+}]/[Fe^{2+}]$ 1:2.5 and 1:2, respectively) the peaks

67º congresso 2012 abm
67th abm international congress
ISSN 1516-392X

shifted to more negative values, approximately -0.72 V, indicating a higher percentage of zinc in the alloy. At these concentrations a complex oxidation process was observed, with the presence of two peaks, around -0.60 V, indicating the formation of phases of the Zn-Fe alloy richer in iron.

Figure 2 shows the galvanostatic dissolution curves for the Zn-Fe coatings obtained under the same conditions, that is, $[Zn^{2+}]$ between 0.10 and 0.40mol/L and −15 mA/cm^2. From baths containing $[Zn^{2+}]$ 0.16 mol/L, 0.18 mol/L and 0.20 mol/L ($[Zn^{2+}]/[Fe^{2+}]$ ratios 1:2,5, 1:2,25 and 2:2, respectively) showed initial values of dissolution potential ranging from -0.80V to -0.91V, characteristic of the presence of phases rich in zinc. The shift of these potentials to about -0.66 V, at the end of the curves indicates the presence of phases with a higher content of iron in the alloy. For the $[Zn^{2+}]$ 0.13 mol/L and 0.10 mol/L the coatings dissolved in near-constant potentials of the order of 0.69 V, indicating a higher content of iron in the Zn-Fe alloy. When the $[Zn^{2+}]$ is high (0.40 mol/L) the dissolution occurs at the 0.90 V, almost constant, typical of zinc-rich phase. The galvanostatic dissolution curves also showed that, in general, increasing the content of zinc in the alloy results in increased efficiency of cathode current. Alloys richer in zinc, with the exception of the alloy obtained for $[Zn^{2+}]$ 0.40 mol/L, showed cathodic efficiency of about 80%, while alloys with higher content of iron, efficiency was approximately 58%, calculated from the ratio of charges Q_{diss}/Q_{dep}, obtained from galvanostatic dissolution curves (Q_{diss}) and used in electroplating (Q_{dep}).

With increasing of the electrodeposition current density from -15 mA/cm^2 to -20 mA/cm^2 (Figure 3) there is a shift of the current peaks to more positive values, close to the potential of pure iron, for the $[Zn^{2+}]$ 0.18 mol/L and 0.20 mol/L, characterized by complex I/E profiles with two current peaks, situated at -0.70 V and -0.60 V. This behavior indicates that the increase in current density favors the formation of the phase with higher content of iron. The obtained results of the galvanostatic dissolution curves also showed the same trend.

Morphological Characterization

In the analysis of the morphology of the electrodeposits of Zn-Fe alloys obtained for different $[Zn^{2+}]/[Fe^{2+}]$ in the electrodeposition bath, it was observed that the grains became increasingly refined until they appeared apparently amorphous, when $[Zn^{2+}]$ 0.10 mol/L. For a higher content of zinc (0.40 mol/L) visibly hexagonal crystals were obtained similar to the morphology of the pure zinc (Figure 4a), which agrees with Gómez, which states that the structure of the electrodeposits with up to 6% iron is similar to that of pure zinc (6).

In Figure 4b, the micrography of the electrodeposits obtained from the bath containing 0.20 mol/L Zn^{2+} showed better coverage of the substrate, with a slight decrease in the size of the crystals, while still maintaining hexagonal appearance. The decrease of the $[Zn^{2+}]$ to 0.18 mol/L in the bath, Figure 4c, resulted in electrodeposits with even smaller crystals. This image shows the loss of the hexagonal structure. When the $[Zn^{2+}]$ in the bath was reduced to 0.16 mol/L, Figure 4d, the morphology of the crystals takes cubic aspect and remains to $[Zn^{2+}]$ 0.13 mol/L, Figure 4e, and a light refinement of this structure is observed.

In Figure 4f, the electrodeposit obtained from the bath containing 0.10 mol/L Zn^{2+} appeared smooth, without a defined crystalline structure, with the presence of cracks, due to the presence of internal stresses in coating. Therefore, the change in morphology and the refinement of the structure can be attributed to the increase in iron content in the deposit. This change results from the relative increase in the

concentration of Fe^{2+} due to the decrease in concentration of Zn^{2+} in the electroplating solution which favors higher nucleation on the electrode surface and consequent reduction of crystal size.
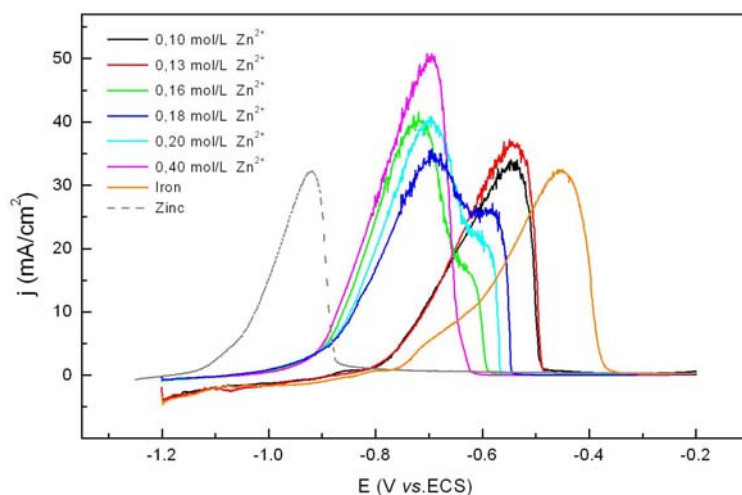
Figure 1 - Dissolution voltammograms for the electrodeposits obtained at -15 mA/cm^2 for different [Zn^{2+}]/[Fe^{2+}] in the electroplating bath. 0.5 mol/L Na$_2$SO$_4$ + 0.05 mol/L EDTA solution.
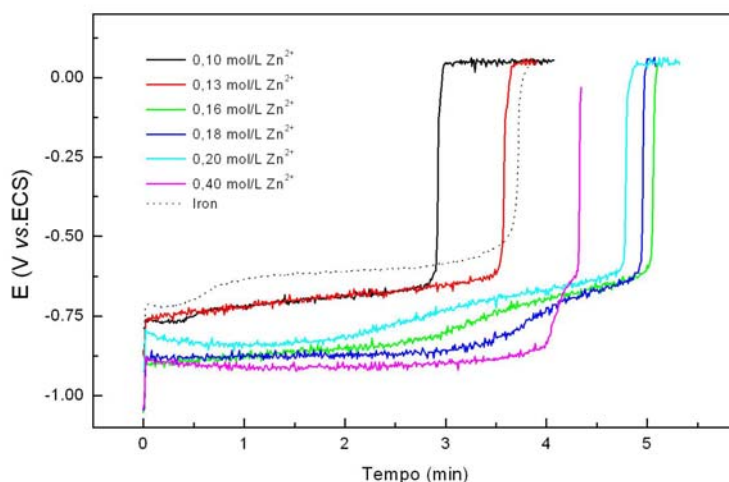
Figure 2 - Galvanostatic dissolution curves for the electrodeposits obtained at -15 mA/cm^2 for different [Zn^{2+}]/[Fe^{2+}] in the electroplating bath. 0.5 mol/L Na$_2$SO$_4$ + 0.05 mol/L EDTA solution.
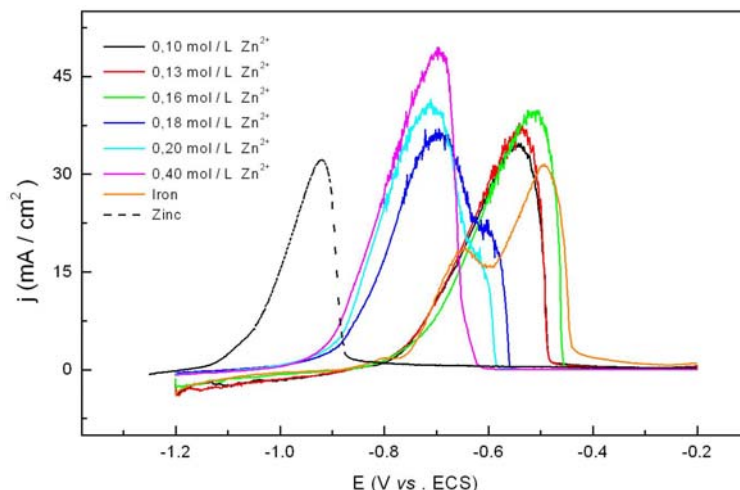
Figure 3 - Dissolution voltammograms for the electrodeposits obtained at -20 mA/cm^2 for different [Zn^{2+}]/[Fe^{2+}] in the electroplating bath. 0.5 mol/L Na_2SO_4 + 0.05 mol/L EDTA solution.

Gómez et al.(6) also observed that the grains of the electrodeposits of Zn-Fe alloy become progressively finer when there is an increase in the amount of iron in the electrodeposits.

(a)

(b)

(b)

(d)

Element	Atom%	Weight%
Zn	79.5	82.0
Fe	20.5	18.0

(e)

Element	Atom%	Weight%
Zn	40.0	43.9
Fe	60.0	56.1

(f)
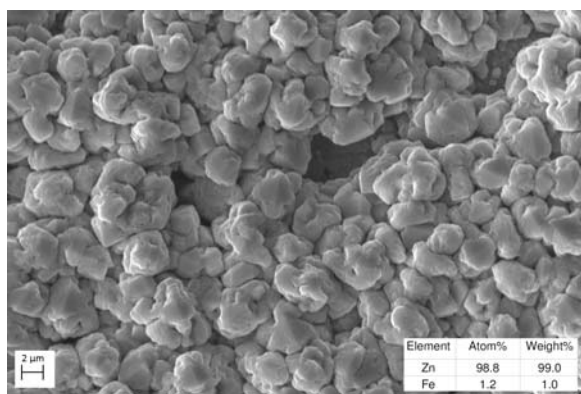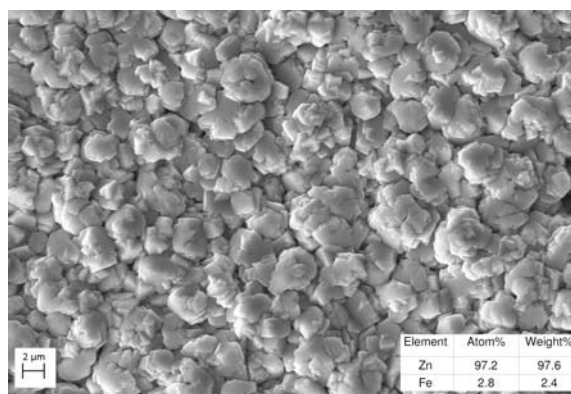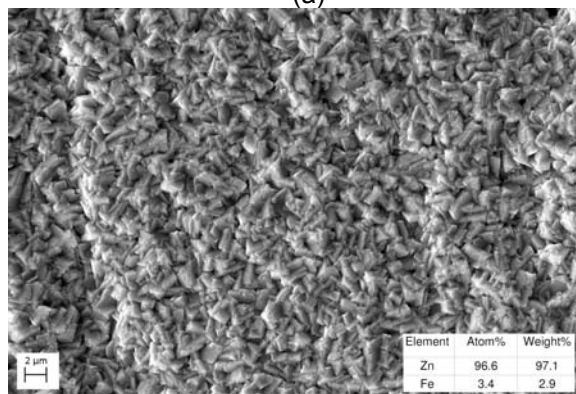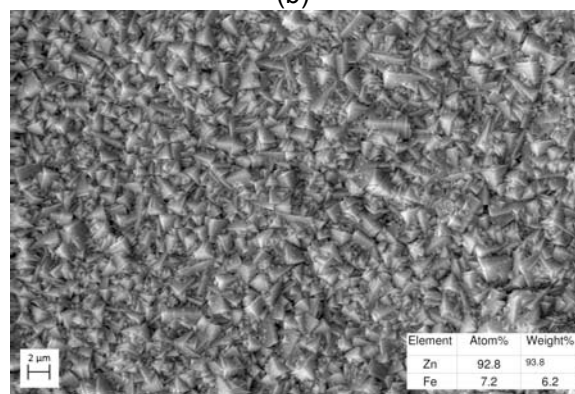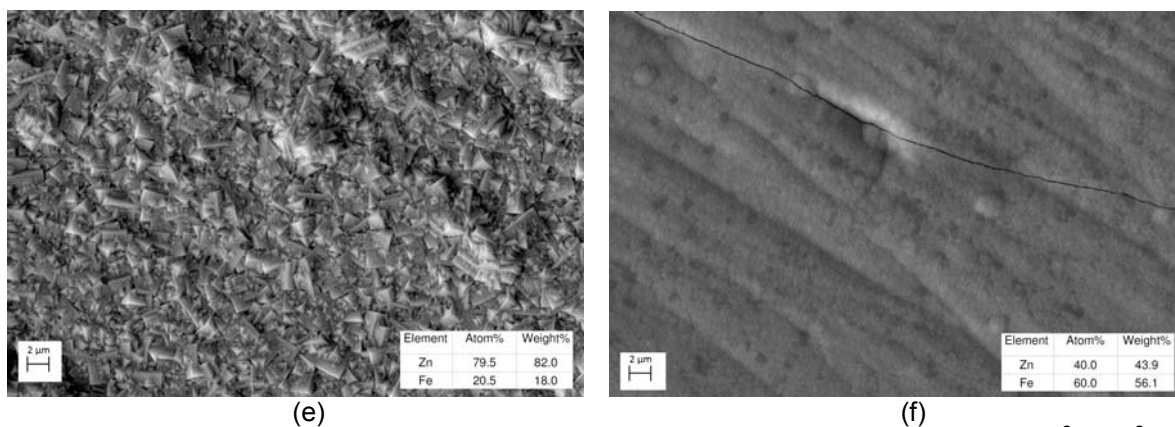
Figure 4 – SEM images and EDS analysis of the electrodeposits obtained for different $[Zn^{2+}]/[Fe^{2+}]$ in electroplating bath. $[Fe^{2+}]$ 0.40 mol/ L, [citrate] 0.10 mol/L and $[Zn^{2+}]$: (a) 0,40 mol/L; (b) 0,20 mol/L; (c) 0,18 mol/L; (d) 0,16 mol/L; (e) 0,13 mol/L; (f) 0,10 mol/L.

X-ray Diffraction

The samples of Zn-Fe alloys analyzed by X-ray diffraction were obtained from electrodeposition baths whose concentration of Fe^{2+} and of citrate were fixed in 0.40 mol/L and 0.10 mol/L, respectively, and the concentration Zn^{2+} varied from 0.10 mol/L to 0.40 mol/L.

Figure 5 shows a series of XRD patterns obtained from the Zn-Fe electrodeposits prepared on the copper substrate, from baths containing different concentrations of Fe^{2+}. In the same figure the composition of the electrodeposits obtained by EDS analysis is shown. When the atomic percentage of iron was 1.2%, the diffractogram showed the following peaks situated at 2θ: 36.6º, 38.4º, 54.4º, 70.4º. The comparison of these peaks with the literature patterns indicates a structure similar to pure Zn, however there are slight displacements and/or extension of the peaks, indicating that the presence of a small amount of iron in the crystalline structure of the Zn promotes a distortion of its lattice parameters.
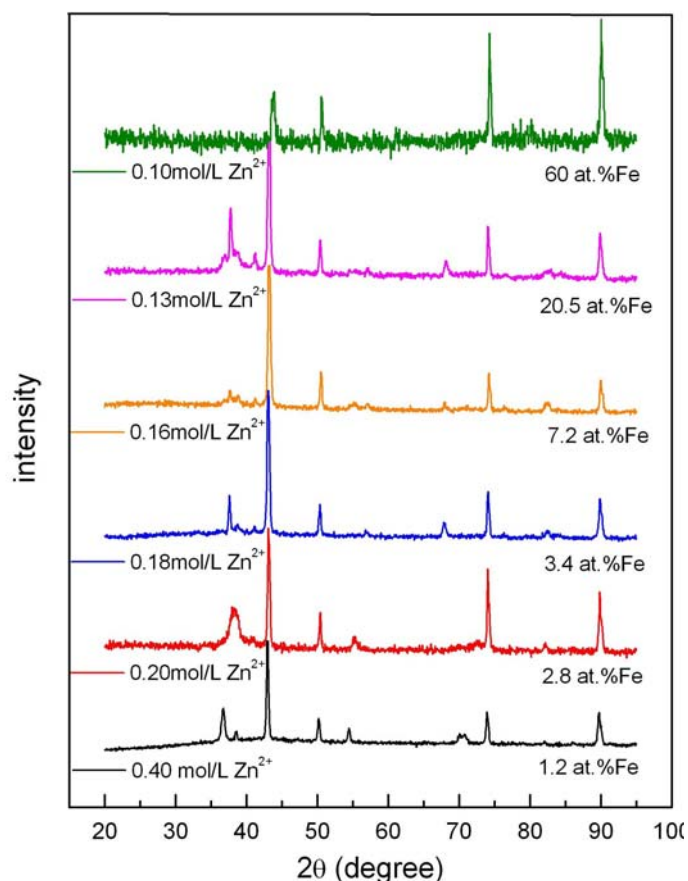
Figure 5 –XRD patterns of electrodeposits of Zn-Fe alloys obtained at -15 mA/cm^2, from electroplating bath containing 0.40 mol/L Fe^{2+}, 0.10 mol/L citrate and different [Zn^{2+}].

In the sample containing 2.8 at.%Fe was observed the disappearance of peaks situated at 2θ 36.7º and 38.5^o respectively, concomitant with the appearance of a broad peak at 2θ 38.2º. The increase in iron content in the alloy results in the appearance of a new peak positioned at 2θ 37.7º which remains up to 20.5 at.%Fe. The latter peak becomes more defined while it increases from 2.8 to 20.5 at.%Fe. Samples containing 3.4 to 20.5 at.%Fe showed peaks situated at 2θ 36.7^o and 38.5^o slightly displaced to 36.8^o and 38.2^o respectively. From 2.8 at.%Fe in the Zn-Fe alloy, a new peak at 2θ at 41º was also observed. At the percentage of 2.8 at.%Fe there was a peak at 2θ 55º which disappeared when the percentage of iron increased to 3.4%, and then, a little pronounced peak located at 2θ 57º appeared. In addition, at 2.8 at.%Fe, a peak appeared at 2θ 68º which remained up to 20.5at.%Fe.

At higher percentages of iron, a peak appeared at 2θ 82.5º, with the exception of the sample containing 60 at.%Fe. The coating containing very high iron content, as in the latter case, shows low crystallinity, that is, it was not possible to observe peaks related to the ZnFe phases, but only the XRD pattern of copper. Copper shows lines at 2θ 43.2º, 50.4º, 74.3º and 90º.

According to Gómez et al.(6), the changes observed in the diffractogram, when small amounts of iron is incorporated into the structure of the zinc are indicatives of the presence of the phase η-ZnFe, the main phase in the Zn-Fe alloy, which is the η-hexagonal of zinc, distorted as a result of the incorporation of iron in the crystal lattice of zinc. These authors also attribute the presence of a possible Zn-Fe phase with a cubic structure of centered face, cfc, in Zn-Fe alloys with high iron content.

The diffractograms of the Zn-Fe alloys containing iron content greater than 3.4 at.%Fe show patterns, which are common, indicating the presence of new Zn-Fe

67º congresso 2012 abm
67th abm international congress
ISSN 1516-392X

phases richer in iron, but which could not be identified because they do not coincide with the phases present in the Zn-Fe alloys obtained by melting. The difficulty in characterizing these phases may be related to the formation of metastable structures, with patterns distinct from those observed in equilibrium conditions.

Study of electrodeposits of Zn-Fe-Co alloys

The study of electrodeposits of Zn-Fe-Co alloys was also performed using electrochemical techniques, SEM/EDS and XRD, for the coatings obtained from the various baths and electrodeposition containing the same concentrations of Zn^{2+}, Fe^{2+} and citrate, but with the addition of 0.05 mol/L Co^{2+} on copper substrate. The study of the influence of the current density was performed by electrolysis in -5 mA/cm^2, -15 mA/cm^2 and -30 mA/cm^2.

Electrochemical study

The analysis of the voltammograms of the anodic dissolution for the electrodeposits obtained in galvanostatic mode at -15 mA/cm^2 (Figure 6), to the highest $[Zn^{2+}]$ (0.40 mol/L) showed a complex process with two peaks, of dissolution, the former being situated at -0.76 V (I), close to the zinc potential, with large charge and a second peak with a smaller charge, close to the iron potential (-0.45 V), region (II). For the intermediate $[Zn^{2+}]$ (0.20 mol/L, 0.18 mol/L, 0.16 mol/L and 0.13 mol/L), a complex dissolution process was always present, with three current peaks situated about -0.79 V (I), 0.57 V (II) and 0.47 V (III), respectively. For the lowest $[Zn^{2+}]$ (0.10 mol/L) only one current peak is observed, at around -0.56 V (II) and a small current shoulder situated at -0.47V (III). The regions (I), (II) and (III) correspond to the potential where the dissolution process is observed of the phases rich in zinc, iron and cobalt, respectively.

Increasing the current to -15 mA/cm^2 the peaks relating to 0.10 mol/L and 0.13 mol/L $[Zn^{2+}]$ shifted to the region of dissolution of iron, both situated at -0.49 V (III), differing only in the charge, the highest one being for the 0.13 mol/L Zn^{2+}. For the 0.16 mol/L Zn^{2+}, a complex peak appeared situated at potentials -0.46 V (III) and -0.54 V (II), respectively. For the higher $[Zn^{2+}]$ (0.18 mol/L, 0.20 mol/L and 0.40 mol/L) there were very similar curves with three well-defined current peaks situated at -0.77 V (I), -0.56 V (II) and -0.47 V (III).

When the electrolysis was carried out at -30 mA/cm^2, only the curve for the 0.40 mol/L Zn^{2+} did not shift to the region of the potential of iron dissolution, showing a peak at -0.73V (I) and a small peak at -0.46V (II). For 0.10 to 0.20 mol/L Zn^{2+}, the peak appeared at -0.48 V (III), confirming that increasing the current applied to the system favors the deposition of iron.

Morphological characterization and X-ray diffraction analysis

Figures 9 -11 show micrographs of the surfaces Zn-Fe-Co alloy and their X-ray diffractograms for electroplating baths containing 0.40 mol/L Fe^{2+}, 0.10 mol/L citrate and the following $[Zn^{2+}]$: 0.40 mol/L, 0.20 mol/L and 0.13 mol/L. The morphology of the alloy obtained from 0.40 mol/L Zn^{2+} (Figure 9a) shows a structure different from that obtained for the Zn-Fe in the absence of Co. The presence of 1.2 at.%Fe and 1.8at.% Co in the alloy results in a globular structure.

The electrodeposits obtained from baths containing $[Zn^{+2}]$ lower show a reduction in size of the crystals as a result of incorporation of a higher content of the Fe and Co (Figures 10a and 11a). For 0.20 mol/L Zn^{2+} was observed an alloy composition of 4.9 at.%Fe and 2.5 at.%Co.

The X-ray diffractogram of the alloy containing 1.2 at.%Fe and 1.8at%Co (Figure 9b) showed the presence of η-phase ZnFe attributed to the peaks at 2θ: 38.6°, 55.2°, 69.9° and 82.2°. The enhanced content 1.2 to 4.9at.%Fe and 1.8 to 2.5at.%Co in the alloy also revealed the presence of η-ZnFe phase identified by X-ray diffractogram (Figure 10b), in which observes the peaks located at 2θ: 36.8°, 38.8°, 54.6°, 70.4°, 77.4°, 82.2° and 86.2°. The appearance of the peak a t 2θ 41.4°, similar to that observed in the Zn-Fe alloy and broad peak coincident with the copper substrate at 2θ 43.2° can be related to the presence of a new phase in the alloy.

The X-ray diffraction patterns obtained for the Zn-Fe-Co were similar to those observed for the Zn-Fe alloy (Figure 5), indicating that incorporation of Co in the structure Zn alloy has a similar effect to that of Fe.

When the $[Zn^{2+}]$ in the bath decreases to 0.13 mol/L, large quantities of Fe(54.3at.%) and Co(7.0at.%) are present in the coating, there is a low crystallinity, as can be seen in the diffractogram of Figure 11b. The X-ray diffractogram for this alloy still shows evidence of the η-ZnFe phase (2θ = 38.6°).

In general, it is noted that the addition of Co^{2+} to electroplating bath favors the incorporation of iron to the Zn-Fe-Co alloy. The Fe content in the ternary alloys is greater than that observed for the binary alloys Zn-Fe when prepared from baths containing the same concentrations of Fe^{2+} and Zn^{+2}, by adding only 0.05 mol/L of Co^{2+}.

4 CONCLUSIONS

The decrease of Zn^{+2} in the electroplating bath results in Zn-Fe electrodeposits with higher Fe content (1.2 – 60at.%) when the ratio $[Zn^{2+}]$: $[Fe^{2+}]$ varies from 1:1 to 1:4. The increase in iron content in Zn-Fe alloy has resulted in the refinement of grain, the morphology of crystals changes from hexagonal to cubic and the structure of the alloy becomes amorphous for the composition near 50 at.%Fe. Zn-Fe alloys with low iron content had a phase rich in zinc (Zn-Fe η-phase). The addition of 0.05 mol/L of Co^{2+} to the electroplating bath for different $[Zn^{+2}]$ and $[Fe^{+2}]$ favor the incorporation of iron in the Zn-Fe-Co alloy. It was also observed that increasing the current density of -5 to -30 mA/cm^2 contributed to the increasing content of Fe in the alloy.
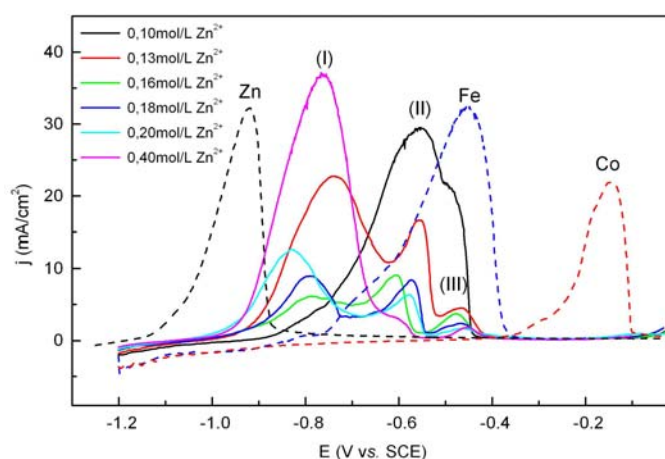
Figure 6– Dissolution voltammograms for the electrodeposits of Zn-Fe-Co alloy obtained at –5 mA/cm^2 for different $[Zn^{2+}]$ in the electroplating bath.
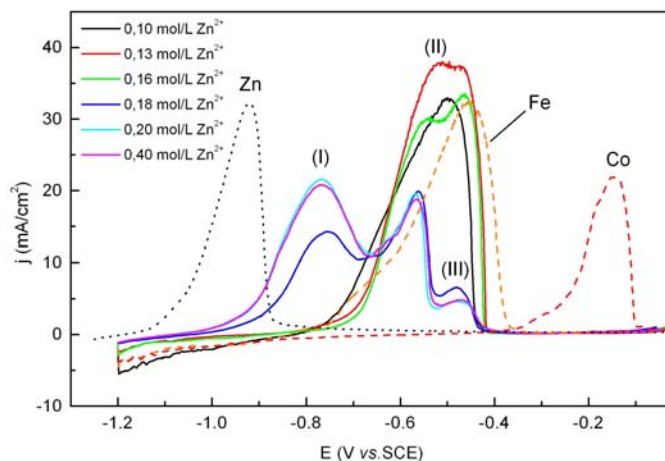
Figure 7– Dissolution voltammograms for the electrodeposits of Zn-Fe-Co alloy obtained at -15mA/cm^2 for different [Zn^{2+}] in the electroplating bath.
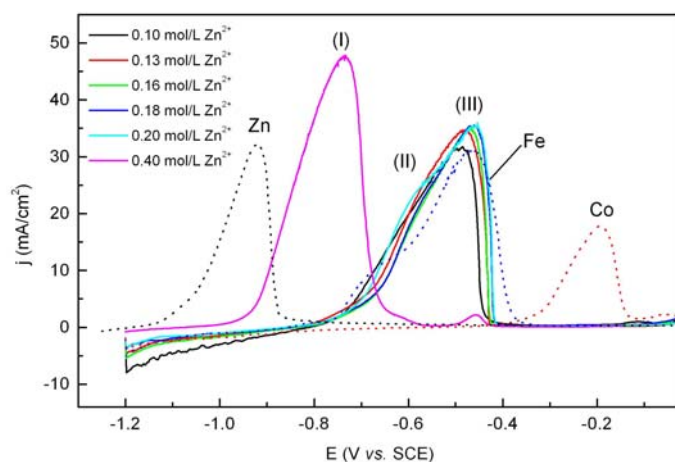
Figure 8– Dissolution voltammograms for the electrodeposits of Zn-Fe-Co alloy obtained at -30mA/cm^2 for different [Zn^{2+}] in the electroplating bath.
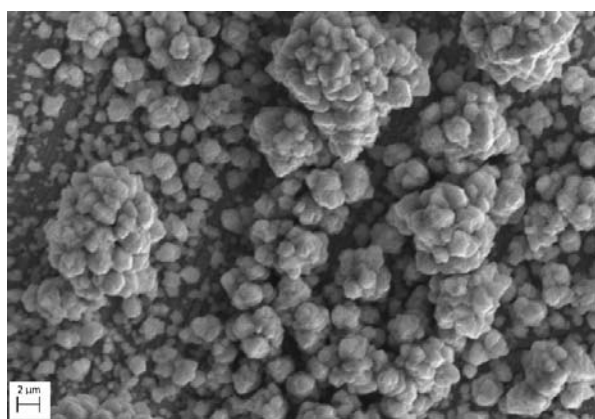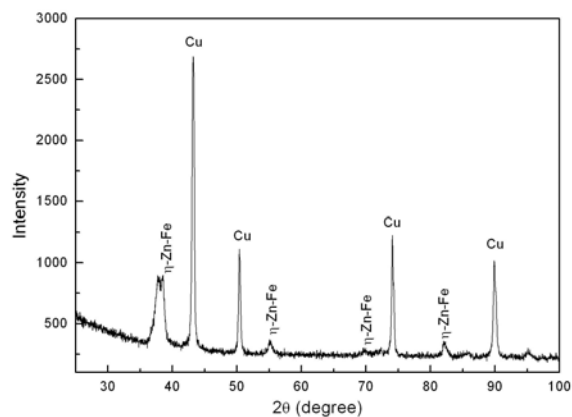
(a)   (b)

Figure 9 – (a) SEM images and (b) XRD patternf the Zn-Fe-Co alloy obtained from electroplating bath containing 0.40 mol/L Fe^{2+}, 0.10 mol/L citrate and 0.40 mol/L Zn^{2+}.
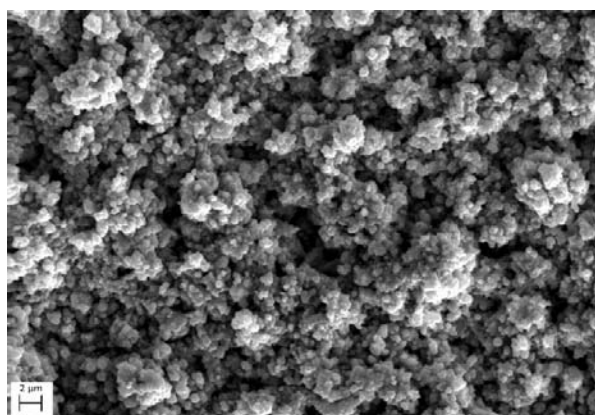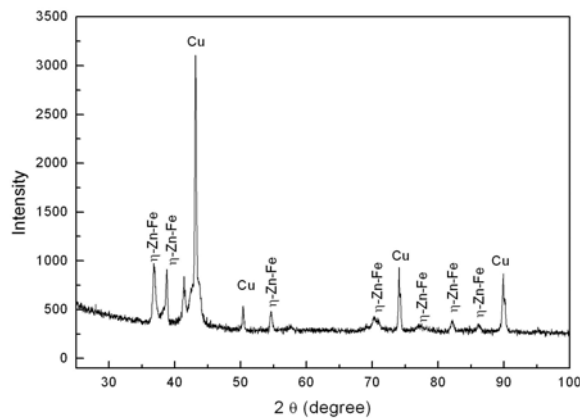
Figure 10 – (a) SEM images and (b) XRD pattern of the Zn-Fe-Co alloy obtained from electroplating bath containing 0.40 mol/L Fe^{2+}, 0.10 mol/L citrate and 0.20 mol/L Zn^{2+}.
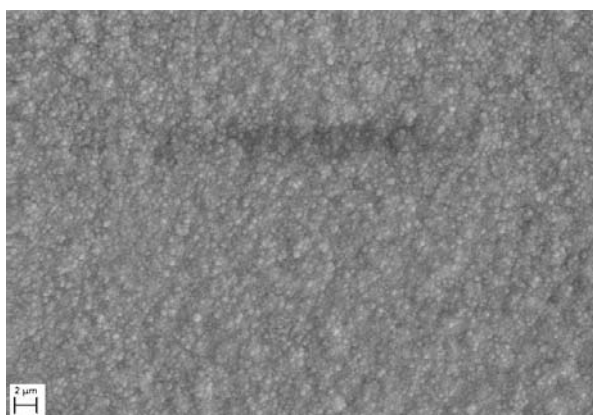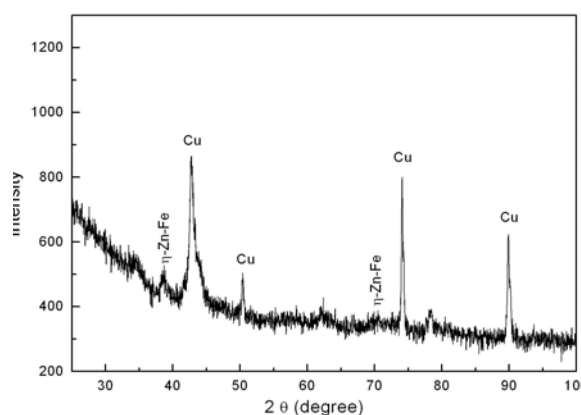
Figure 11 – (a) SEM images and (b) XRD pattern of the Zn-Fe-Co alloy obtained from electroplating bath containing 0.40 mol/L Fe^{2+}, 0.10 mol/L citrate and 0.13 mol/L Zn^{2+}.

Acknowledgements

REFERENCES

1 LODHI, Z. F.; MOL, J. M. C.; HOVESTAD, A. ; TERRYN, H. ; WIT, J. H. W. Corrosion Resitance of Zn-Co Alloy Coatings on High Strength Steel. Surface & Coatings Technology, v.203, p.1415-1422, 2009.
2 LODHI, Z. F. ; MOL, J. M. C. ; HOVESTAD, A. ; TERRYN, H. ; WIT, J. H. W. Eletrodeposition of Zn-Co and Zn-Co-Fe alloys from acidic chloride electrolytes. Surface & Coating Technology, v. 202, p.84-90, 2007.
3 NETO L.P.; SOUZA, A.O.; NOGUEIRA, M.I.C.; COIARES, R.P. Estudos da Corrosão de Eletrodepósitos de ZnNi, ZnFe e ZnCo em meio de cloreto e de sulfato. In: 6º COTEQ, Salvador, 2002.
4 BAJAT, J. B.; MISKIVIC-STANKOVIC, V. B.; MAKSIMOVIC, M. D.; DRAZIC, D. M., ZEC, S. Electrochemical deposition and characterization of Zn-Co alloys and corrosion protection by electrodeposited epoxy coating on Zn-Co alloy. Electrochimica Acta, v.47, p. 4101-411, 2002.

5   LODHI, Z. F.; TICHELAAR, F.D.; KAWAKAERMAAK, C.; MOL, J. M. C.; TERRYN, H.; WIT, J. H. W. A combined composition and morphology study of electrodeposited Zn-Co and Zn-Co-Fe alloys coatings. Surface & Coating Technology, v. 202, p.2755-2764, 2007.
6   GÓMEZ, E; ALCOBE, X; VALLÉS. E.   Electrodeposition of zinc + iron alloys. II. Relation between the stripping results and ex-situ characterization. Journal of Electroanalytical Chemistry, Barcelona, v.475, p.66-72, 1999.
7   BRENNER, A. **Electrodeposition of alloys, principles and practice**. Vol. I. New York: Academic Press, 1963.
8   GÓMEZ, E.; ALCOBE, X.; VALLÉS, E. Characterization of zinc + cobalt alloy phases obtained by electrodeposition. Journal of Electroanalytical Chemistry,   v. 505, p. 54-61, 2001.
9   SIKORA, E.; MacDONALD, D.D. The passivity of iron in the presence of ethylenediaminetetraacetic. I. General electrochemical behavior. Journal of the Electrochemical Society, v. 147, p. 4087-4092, 2000.